

Effect of Chemical Composition on Curie Temperature of FeCoB Alloys

M. NABIAŁEK^a, B. JEŹ^a, P. PIETRUSIEWICZ^a, K. JEŹ^a,
B. PŁOSZAJ^a, A.V. SANDU^{b,c}, M.M.A.B. ABDULLAH^b,
J. WYSŁOCKI^a, A. KALWIK^d,
P. POSTAWA^d AND M.A.A. MOHD SALLEH^b

^a*Department of Physics, Faculty of Production Engineering and Materials Technology, Częstochowa University of Technology, al. Armii Krajowej 19, 42-200 Częstochowa, Poland*

^b*Center of Excellence Geopolymer & Green Technology (CeGeoGTech), Faculty of Chemical Engineering Technology,*

Campus Dragon, Complex Pusat Pengajian Jejawi 3, 02600 Arau, Perlis, Malaysia

^c*Faculty of Materials Science and Engineering, Gheorghe Asachi Technical University of Iasi, Blvd. D. Mangeron 41, 700050 Iasi, Romania*

^d*Department of Technology and Automation, Faculty of Mechanical Engineering and Computer Science, Częstochowa University of Technology, al. Armii Krajowej 19, 42-200 Częstochowa, Poland*

Doi: [10.12693/APhysPolA.139.491](https://doi.org/10.12693/APhysPolA.139.491)

*e-mail: nmarcell@wp.pl

This paper presents the results of research on saturation magnetic polarisation, as a function of temperature, for a group of rapidly-cooled FeCoB alloys. The tested alloys have soft magnetic properties. Thermal stability, as determined by the Curie temperature, is one of the most important parameters for classifying the use of magnetic materials. In this work, the Curie temperature values for selected alloys were determined, using the critical factor of $\beta = 0.36$. The area under each saturation magnetic polarisation curve, and the shape of the curve itself, were also analysed. It was found that even small changes in the chemical composition of the alloy can lead to a shift in the temperature that marks the boundary between the ferromagnetic and paramagnetic states.

topics: rapidly-quenched alloys, X-ray diffractometry, Curie temperature, injection-casting method

1. Introduction

The Curie temperature is one of the most important parameters describing ferromagnetic materials — it determines the stability of the ferromagnetic state, and more precisely the stability of the existence of magnetic domains. When the temperature is high enough for disappearance of the domains in a ferromagnetic material, a second form of phase transition will begin and the material becomes paramagnetic. Nowadays, there is considerable interest in rapidly-cooled amorphous materials as ferromagnetic alloys with unique magnetic properties [1–4].

Methods based on the rapid cooling of liquid alloy made possible the manufacture of products of various shapes and thicknesses. The obvious fact is that it is easiest to produce amorphous alloys of small cross-sectional thickness. The first ferromagnetic amorphous materials were produced in the form of thin layers and thin ribbons [5]. Obtaining thin layer samples is a laborious, time-consuming

task and requires expensive specialised equipment. On the other hand, the production of ribbons using the method involving unidirectional cooling of liquid alloy on a rotating copper cylinder (i.e., melt-spinning [6]) is simple, does not require much time and is also relatively cost-effective. The possible cooling rates, obtained during melt-spinning, range around 10^4 – 10^6 K/s. The obtained ribbons can have thicknesses ranging between 12 μm to maximally 100 μm , while still maintaining their integrity.

Simple measurements can show that such ribbons can operate effectively at very high frequencies [7]. Therefore, they started to be used as a basis for the magnetic cores of transformers. However, the air gaps formed during their “packaging,” effectively render them unsuitable for operation at high frequencies. This is due to the emission of excessive noise and overheating. As a result, research progressed into theoretical foundations and methods for the production of greater thicknesses

of amorphous materials. In 1989, A. Inoue of the University of Tohoku, and his colleagues, presented three empirical principles enabling the production of amorphous materials with thicknesses significantly exceeding 100 μm . It was noted then that the introduction of more than three components to the composition of an alloy reduces the migration of atoms within the alloy and the formation of energetically favoured systems characterised by long-range interactions between atoms. The researchers also found that the selection and maintenance of appropriate differences between the atomic radii of the alloying elements, and with negative mixing heat, causes an increase in viscosity during solidification of the alloy and concomitant blockage of the movement of atoms [8, 9]. From 1989, a new era of amorphous materials began, resulting in a new group called the bulk amorphous materials. Obtaining bulk amorphous materials on an FeCoB matrix is a difficult task and the obtained thicknesses are much smaller than, for example, those for alloys based on a Pd or Zr matrix [10–16].

This paper presents the results of research on the saturation magnetic polarisation, as a function of temperature, for bulk amorphous alloys based on an FeCoB matrix.

2. Experimental procedure

The samples for this research were prepared from high purity component elements: Fe — 99.99; Co — 99.99; Y — 99.95; B — 99.9. Component elements were weighed to four decimal places and used to prepare crystalline ingots. The ingots were melted, under an inert gas atmosphere, in electric arc furnace. Bonding of the alloying elements was carried out on a water-cooled copper plate by using a plasma arc with an operating current of 350 A. After the first melting of the alloy, the chamber was cleaned and the ingot was re-melted under the same conditions several times — four times on each side. During the process, titanium was pre-melted to act as an absorbent for the remaining oxygen in the chamber. After the homogenisation cycle, each alloy sample was subjected to both mechanical and ultrasonic cleaning. The ingots were then divided into smaller batch portions for the production of amorphous samples of liquid alloy injected into a copper mould. A piece of each respective alloy was placed into a quartz capillary tube and melted using induction heating; the liquid alloy was then injected under argon pressure into a water-cooled copper mould. The rapidly-cooled samples were also produced under a protective gas shield inside the working chamber. The produced samples were in the form of plates with an area of $10 \times 10 \text{ mm}^2$ and a thickness of 0.5 mm.

X-ray (XRD) examinations were performed on samples in the solidified state using a BRUKER D8 ADVANCE X-ray diffractometer ($\text{CuK}\alpha$). The samples were scanned over a 2θ angle range from 30°

to 100° with a measurement step of 0.02° and with a time per step of 7 s. Measurements of magnetic polarisation, as a function of temperature, were obtained using a Faraday magnetic scale. The samples were heated at a rate of 10 K/min. Measurements were made, under a vacuum, for samples weighing 25 mg. The magnetic field intensity during the measurement was 0.7 T and the maximum measurement temperature, determining the stability of the measurement system, was 850 K. Both the XRD and thermomagnetic measurements were made on low-energy powdered samples (0.1 m). The test samples were pulverised (under toluene) manually, using an agate mortar.

3. Results

Figure 1 presents X-ray diffraction images obtained for the tested alloys in the solidified state. The obtained diffraction patterns consist of only one broad maximum which is within the 2θ angle range from 40° to 50° . A background with low intensity was visible in the higher range of the diffraction pattern. Such X-ray diffraction patterns are typical for materials with an amorphous structure. The thermomagnetic properties of the alloys were analysed on the basis of the saturation magnetic polarisation, as a function of temperature T (Fig. 2). Each thermomagnetic curve presented in Fig. 2 has a typical shape for an amorphous material, and is characterised by a single Curie temperature. Based on analysis of the presented curves, it can be concluded that none of the tested alloys crystallised within the tested temperature range. Additionally, it can be concluded that there were no areas characterised by long-range order, within the volume of the tested alloys. This is because, in the region of the transition from the ferromagnetic to the paramagnetic state, the magnetisation was reduced to near zero.

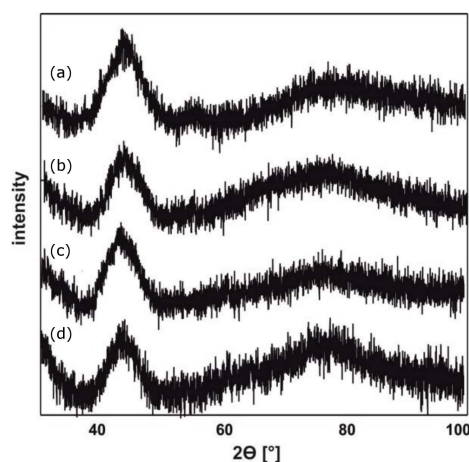


Fig. 1. X-ray diffraction patterns for the investigated alloys rod-form samples: (a) $\text{Fe}_{36}\text{Co}_{36}\text{Y}_8\text{B}_{20}$, (b) $\text{Fe}_{39}\text{Co}_{43}\text{Y}_8\text{B}_{20}$, (c) $\text{Fe}_{43}\text{Co}_{29}\text{Y}_8\text{B}_{20}$, and (d) $\text{Fe}_{48}\text{Co}_{24}\text{Y}_8\text{B}_{20}$.

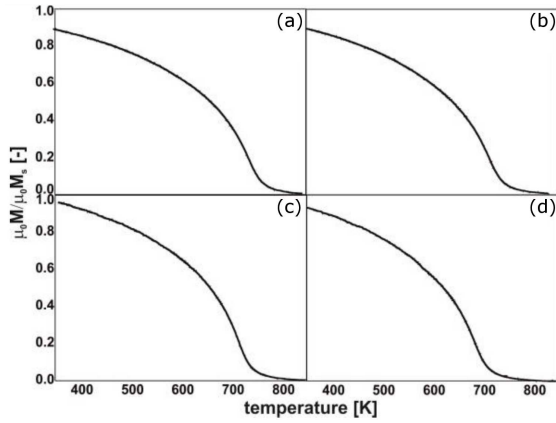


Fig. 2. Thermomagnetic curves obtained for the tested alloy samples: (a) $\text{Fe}_{36}\text{Co}_{36}\text{Y}_8\text{B}_{20}$, (b) $\text{Fe}_{39}\text{Co}_{43}\text{Y}_8\text{B}_{20}$, (c) $\text{Fe}_{43}\text{Co}_{29}\text{Y}_8\text{B}_{20}$, (d) $\text{Fe}_{48}\text{Co}_{24}\text{Y}_8\text{B}_{20}$ in the solid state.

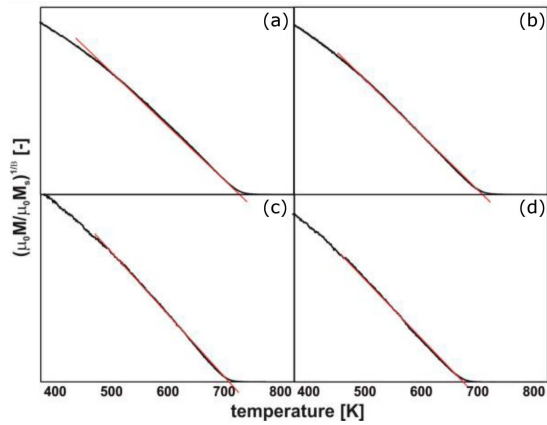


Fig. 3. Relationship of $(\mu_0 M)^{1/B}$ with temperature T , for the tested alloys: (a) $\text{Fe}_{36}\text{Co}_{36}\text{Y}_8\text{B}_{20}$, (b) $\text{Fe}_{39}\text{Co}_{43}\text{Y}_8\text{B}_{20}$, (c) $\text{Fe}_{43}\text{Co}_{29}\text{Y}_8\text{B}_{20}$, (d) $\text{Fe}_{48}\text{Co}_{24}\text{Y}_8\text{B}_{20}$ in the state after solidification.

The analysed samples meet Heisenberg's assumptions and it was possible to apply the critical factor, equal to 0.36, to them. Figure 3 shows $(\mu_0 M)^{1/B}$ curves as a function of T , and linear adjustments enabling the determination of the Curie temperature values. The relationship presented confirms the earlier assumptions that there is only one Curie temperature in the tested materials. Data obtained from analysis of the X-ray diffraction patterns, the saturation magnetic polarisation curves — as a function of temperature — and the relationship $(\mu M)^{1/B}(T)$ are presented in Table I.

4. Conclusions

This paper presents the results of research carried out on rapidly-cooled solidified alloy samples, characterised by an amorphous structure. The tested alloys differed slightly in their chemical composition. Structural and thermomagnetic tests were

TABLE I

Results of the research: maximum width of the amorphous halo, Curie temperature T_C , area under the thermomagnetic curve H_K .

	Max. width [°]	T_C [K]	H_K
$\text{Fe}_{36}\text{Co}_{36}\text{Y}_8\text{B}_{20}$	11.8	741	357
$\text{Fe}_{39}\text{Co}_{43}\text{Y}_8\text{B}_{20}$	11.2	717	325
$\text{Fe}_{43}\text{Co}_{29}\text{Y}_8\text{B}_{20}$	11.1	700	301
$\text{Fe}_{48}\text{Co}_{24}\text{Y}_8\text{B}_{20}$	11.0	673	288

performed and the obtained results are typical for amorphous alloys with good homogeneity. The performed changes in the chemical composition affect the width of the amorphous halo, the area under the thermomagnetic curve H_K and the Curie temperature T_C . It should be noted that the Curie temperature in amorphous materials should be described as a very narrow temperature range rather than a discrete value. When designing amorphous alloys for use in electrical engineering, it is important not only that the Curie temperature itself is considered, but also that the shape of the saturation magnetic polarisation curve, as a function of temperature, should be carefully analysed. If this curve does not extend down to zero, it is most likely that there are crystallisation seeds in the amorphous matrix, which will directly affect the process of nanocrystallisation of the amorphous matrix.

References

- [1] F. Wang, A. Inoue, Y. Han, F. Kong, S. Zhu, E. Shalaan, F. Al-Marzouki, A. Obaid, *J. Alloys Compd.* **711**, 132 (2017).
- [2] X. Li, Z. Shi, T. Zhang, *J. Alloys Compd.* **784**, 1139 (2019).
- [3] M.E. McHenry, M.A. Willard, D.E. Laughlin, *Prog. Mater. Sci.* **44**, 291 (1999).
- [4] M. Nabialek, K. Jeż, B. Jeż, *Acta Phys. Pol. A* **135**, 136 (2019).
- [5] W. Klement, R.H. Willens, P. Duwez, *Nature* **187**, 869 (1960).
- [6] M. Nabialek, *Rev. de Chim.* **69**, 2819 (2018).
- [7] A. Masood, H.A. Baghbaderani, K.L. Alvarez, J.M. Blanco, Z. Pavlovic, V. Ström, P. Stamenov, C.O. Mathuna, P. McCloskey, *J. Magn. Magn. Mater.* **519**, 167469 (2021).
- [8] A. Takeuchi, A. Inoue, *Mater. Trans.* **46**, 2817, (2005).
- [9] T. Nagase, M. Suzuki, T. Tanaka, *Intermetallics* |bf 61, 56 (2015).
- [10] H.S. Chen, D. Turnbull, *Acta Metall.* **17**, 1021 (1969).

- [11] Q.K. Jiang, X.P. Nie, Y.G. Li, Y. Jin, Z.Y. Chang, X.M. Huang, J.Z. Jiang, *J. Alloys Compd.* **443**, 191 (2007).
- [12] B.T. Borkar, A.B. Borkar, D. Janardhanan, P. Deshmur, *Eur. J. Mater. Sci. Eng.* **05**, 03 (2020).
- [13] M.S. Baltatu, C.A. Tugui, M.C. Perju, M. Benchea, M.C. Spataru, A.V. Sandu, P. Vizureanu, *Rev. de Chim.* **70**, 1302 (2019).
- [14] P. Rawn, V. Sudhakar, *Eur. J. Mater. Sci. Eng.* **04**, 29 (2019).
- [15] A.V. Sandu, C. Coddet, C. Bejinariu, *J. Optoelectron. Adv. Mater.* **14**, 699 (2012).
- [16] B. Jeż, J. Wysocki, S. Walters, P. Postawa, M. Nabiątek, *Materials* **13**, 1367 (2020).